Suppressing relaxation through dephasing

T. Palm [1,2] and P. Nalbach[1]

[1]*Fachbereich Wirtschaft & Informationstechnik, Westfälische Hochschule, Münsterstrasse 265, 46997 Bocholt, Germany*

[2]*I. Institut für Theoretische Physik, Universität Hamburg, Jungiusstraße 9, 20355 Hamburg, Germany*

(Received 28 October 2019; revised 9 July 2020; accepted 25 January 2021; published 9 February 2021)

We study the nonequilibrium dynamics of a quantum system under the influence of two noncommuting fluctuation sources, i.e., purely dephasing fluctuations and relaxational fluctuations. We find that increasing purely dephasing fluctuations suppress increasing relaxation in the quantum system. This effect is further enhanced when both fluctuation sources are fully correlated. These effects arise for medium to strong primary fluctuations already when the secondary fluctuations are weak due to their noncommuting coupling to the quantum system. Dephasing, in contrast, is increased by increasing any of the two fluctuations. Fully correlated fluctuations result in overdamping at much lower system-bath coupling than uncorrelated noncommuting fluctuations. In total, we observe that treating subdominant secondary environmental fluctuations perturbatively leads, as neglecting them, to erroneous conclusions.

DOI: 10.1103/PhysRevA.103.022206

I. INTRODUCTION

Open quantum dynamics is a very successful approach to describe and treat dissipative effects like relaxation, decoherence, and dephasing in quantum systems [1–4]. Dissipation results therein by coupling the quantum system of interest to an environmental thermal bath. The later is typically described by a set of harmonic oscillators bilinearly coupled to the system. The according system-bath model is treated either perturbatively or by numerical exact methods. Thus, successful treatment of, for example, problems like dephasing in various qubit realizations [5], energy transfer in photosynthetic complexes [6], and quantum tunneling in macroscopic molecular spin clusters [7], to name a few, is enabled.

The studied quantum systems vary widely but a simplified description in terms of a modeling as either harmonic oscillator or two-state system (TSS) is employed in most cases. When their coupling to the bath induces transitions between the system eigenstates, the bath enables relaxation and we term such a bath as *relaxational*. The dynamics of a harmonic oscillator coupled to a relaxational bath can be solved analytically [8]. In contrast, a TSS coupled to a relaxational bath, termed the *spin-boson model* [2,3], cannot be solved analytically. Approximate treatments for the weak and strong coupling limits as well as numerical exact procedures are, however, available. When the coupling to the bath does not induce relaxation, the system dynamics still dephases and we term the according baths as *pure dephasing baths* in the following. A TSS coupled to a pure dephasing bath (termed *independent boson model* [9]) can be solved analytically.

Typically, there is not a single relevant environmental bath but many. Charge and flux qubits, for example, experience noise due to phonons, voltage fluctuations in the various gates, charged defects and currents through nearby quantum point contacts [5,10,11]. Chromophores in photosynthetic complexes are disturbed by strong environmental fluctuations due to intra- and intermolecular vibrations of the photoactive complexes, vibrations of embedding proteins, solvent fluctuations, and the charge separation in the reaction center [6].

Assuming all baths are at the same temperature, then the influences of multiple baths are *additive*, as long as they couple to the quantum system via operators, which commute. The simplest case is when all baths couple to the same operator, for example, the system's dipole operator. Then, all baths can be combined to an effective single bath with combined spectral function. If the baths couple to different but commuting operators, the total influence functional is a simple extension of the well known Feynman-Vernon influence functional for a single bath [12,13]. Terming the influence *additive* means that for weak enough coupling, where the dissipative effects are mainly encaptured in relaxation and dephasing rates, commuting baths result in relaxation and dephasing rates which are given by the sum of the respective rates from each single bath. If, however, the various system operators, which couple to separate environments, do not commute, the resulting noncommuting fluctuations in the system can give rise to peculiar *nonadditive* effects. For example, at zero temperature a suppression of the localization phase transition has been observed [14–16]. Multiple noncommuting baths are treated when studying molecular energy transfer [17–19], i.e., at conical intersections [20–22]. Qubits under the influence of non-commuting fluctuations, however, have not been studied, so far, although, to control a qubit, noisy external forces must couple to various, i.e., explicitly noncommuting system observables.

We determine the nonequilibrium dynamics of a quantum two-state system (TSS) under the influence of two noncommuting baths, i.e., a relaxational and a purely dephasing bath. We compare the results with a case where a single bath couples with the same strengths to both noncommuting system

operators. This later model reflects a situation where both baths are fully correlated instead of uncorrelated as one might expect for independent thermal baths. We employ the numerical exact quasiadiabatic path integral approach (QUAPI) [23–25] which was extended to treat multiple, i.e., noncommuting, baths [13,26,27].

In the next section we introduce the studied model. Section III introduces our observables and how to obtain them from the numerical data. Subsequently, we shortly introduce our employed method before in Secs. V and in Sec. VI we detail our results. We end with a conclusion. Our main finding is that even weak secondary noise sources cannot adequately be treated as an additive influence when multiple environmental noise sources couple to a quantum system via noncommuting operators. Our results are important to achieve a proper characterization of environmental noise sources in experiments.

II. MODEL

We study a symmetric TSS with Hamiltonian

$$H_S = -\frac{\Delta}{2}\sigma_x, \tag{1}$$

coupled to two baths, one, i.e., $H_{SB,z}$, causing relaxational fluctuations due to its coupling via σ_z to the TSS and the other, i.e., $H_{SB,x}$, coupled via σ_x causing pure dephasing fluctuations. This leads to a total Hamiltonian

$$H = H_S + H_{SB,z} + H_{SB,x} \tag{2}$$

with

$$H_{SB,\nu} = \sum_{k=1}^{M} \frac{p_{k,\nu}^2}{2m_{k,\nu}} + \frac{1}{2}m_{k,\nu}\omega_{k,\nu}^2\left(q_{k,\nu} - \frac{\xi_{k,\nu}\sigma_\nu}{m_{k,\nu}\omega_{k,\nu}^2}\right)^2 \tag{3}$$

and $[q_{k',\nu'}, p_{k,\nu}] = i\hbar\delta_{k,k'}\delta_{\nu,\nu'}$. Herein, the $q_{k,\nu}$ and $p_{k,\nu}$ are the position and momentum of mode k with frequency $\omega_{k,\nu}$ of bath ν coupled via $\xi_{k,\nu}$ to the system. The σ_ν are the corresponding Pauli matrices of the TSS algebra by which the corresponding bath fluctuations couple to the TSS. For later convenience we split the coupling $\xi_{k,\nu} = a_\nu\lambda_{k,\nu}$ between system and bath mode in two factors. All relevant information about the baths are captured in the spectral densities,

$$G_\nu(\omega) = \sum_{k=1}^{M} \frac{\lambda_{k,\nu}^2 \cdot \delta(\omega - \omega_{k,\nu})}{2m_{k,\nu}\omega_{k,\nu}} =: \widetilde{\gamma}_\nu \omega e^{-\omega/\omega_c}, \tag{4}$$

chosen here for simplicity as Ohmic spectra with an exponential cut-off function and with $\nu = x$ or $\nu = z$. Therein, ω_c is the bath cut-off frequency chosen to be $\omega_c = 5\Delta$ for both baths. Note that we have not included the mode-independent factor a_ν in the definition of the spectral density and that a_ν will be chosen throughout the work to obtain $\widetilde{\gamma}_\nu = 1$. The coupling strength between the ν fluctuations and the quantum system is $\gamma_\nu = a_\nu^2\widetilde{\gamma}_\nu$.

Our focus is on the question of how far the two baths influence each other and the resulting dissipative effects are not the sum of the two baths individual effects. By choosing the two baths to couple either only to σ_z or to σ_x (instead of bath i coupled via combinations $f_{z,i}\sigma_z + f_{x,i}\sigma_x$) simplifies the analysis of our numerical investigation since for both separate bath the relaxation and dephasing dynamics are well studied. Experimentally, one might observe at which system operator an environmental fluctuating force acts upon. It is, however, rather difficult to decide whether these stem from a single cause or two separate environmental baths. Therefore, we study additionally fully correlated (FC) fluctuations, i.e., $q_{k,x} = q_{k,z} \equiv q_k$ and $p_{k,x} = p_{k,z} \equiv p_k$, where both fluctuations result from a single environmental source, and compare with results for uncorrelated fluctuations (UC), i.e., $[q_{k,x}, p_{k,z}] = 0$, which reflects a case with two independent environmental fluctuation sources.

III. STUDIED OBSERVABLES–DEPHASING AND RELAXATION RATES

We explicitly study the time evolution of $P_z(t) = \langle\sigma_z\rangle(t)$ (which reflects the coherent oscillations of a TSS with Hamiltonian (1) between the σ_z eigenstates) with initially $P_z(0) = 1$ to investigate dephasing and $P_x(t) = \langle-\sigma_x\rangle(t)$ (which reflects the population difference of the two energy eigenstates) with initially $P_x(0) = 1$ to study relaxation. We employ a fitting function $P_z^{\rm fit}(t) = P_z^{\rm stat} + [x_1 + x_3\sin(\widetilde{\Delta}(t)t) + x_2\cos(\widetilde{\Delta}(t)t)]e^{-x_7 t}$ with $\widetilde{\Delta}(t) = (x_4 + x_5 e^{-x_6 t})$ and $P_z^{\rm stat} = 1 - x_1 - x_2$ and with the x_i the fit parameters to describe the numerical data. The fit function reflects the functional form obtained for $P_z(t)$ by an analytical weak coupling approximation [3]. As expected from weak coupling analytical results we observe $|P_z^{\rm stat}| \ll 1$ and $\widetilde{\Delta}(t) \simeq \Delta$ and $x_1, x_3 \ll x_2$ for all studied cases, i.e., $\gamma_x \leqslant 0.5$, $\gamma_z \leqslant 0.5$ and temperatures $0.1\Delta \leqslant k_{\rm B}T \leqslant 2\Delta$. We, thus, extract the dephasing rate $x_7 = \Gamma_d^{\rm (FC)}$ for fully correlated fluctuations or $x_7 = \Gamma_d^{\rm (UC)}$ for uncorrelated fluctuations. The relaxation rate $\Gamma_r^{\rm (FC)}$ and $\Gamma_r^{\rm (UC)}$ are extracted similarly by fitting $P_x^{\rm fit}(t) = P_x^{\rm stat} + (1 - P_x^{\rm stat})e^{-x_8 t}$ to the data and identifying $x_8 = \Gamma_r^{(FC)}$ or $x_8 = \Gamma_r^{(UC)}$ respectively. The fit function is chosen to coincide with the functional form obtained for $P_x(t)$ by an analytical weak coupling approximation [3] focusing on the dominant terms.

These dephasing and relaxation rates are functions of both coupling strength γ_x and γ_z. Note that by fixing $\widetilde{\gamma}_\nu \equiv 1$ and choosing a_x and a_z identical for fully correlated or uncorrelated fluctuations we ensure that in lowest order of the coupling to the bath the dephasing and relaxation rates for the quantum two-state system are identical for fully correlated and uncorrelated fluctuations. All differences result from higher order corrections due to medium to strong system-bath coupling of at least one of the fluctuation sources.

Our model simplifies to the standard spin-boson model (SBM) for $a_x = 0$ or to an independent boson or pure dephasing model (PDM) for $a_z = 0$. To further highlight how correlations modify dissipation we additionally determine the rates of the SBM and the PDM model for the same coupling strength and add them: $\Gamma_{r/d}^{\Sigma} = \Gamma_{r/d}^{\rm PDM}(\gamma_x, \gamma_z = 0) + \Gamma_{r/d}^{\rm SBM}(\gamma_x = 0, \gamma_z)$. This rate would result if the bath influences would be additive.

IV. METHOD

To determine the nonequilibrium dynamics of the TSS under the influence of two baths, we employ the QUAPI approach [26] originally developed for a single bath case [23–25]. Analytical strong coupling approaches like the Niba

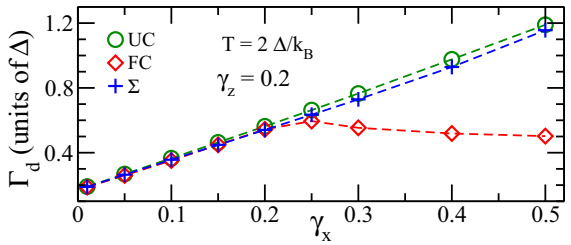

FIG. 1. The dephasing rates $\Gamma_d^{(FC)}$ for fully correlated (red diamonds) and $\Gamma_d^{(UC)}$ for uncorrelated (green circles) fluctuations and Γ_d^{Σ} (blue plus symbols) are plotted versus the coupling strength for the dephasing fluctuations γ_x for a fixed $\gamma_z = 0.2$ and a high temperature $T = 2\Delta/k_B$.

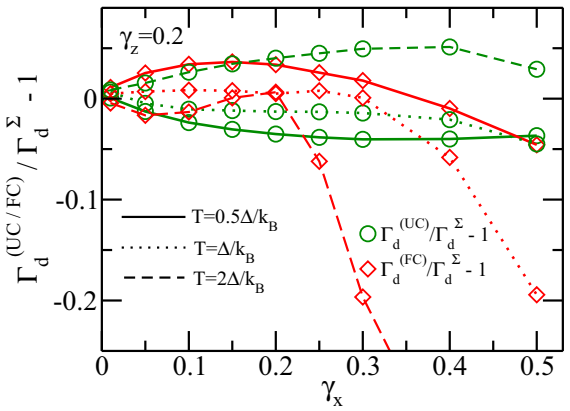

FIG. 2. The ratio $(\Gamma_d^{(FC)} - \Gamma_d^{\Sigma})/\Gamma_d^{\Sigma}$ for fully correlated (red diamonds) and $(\Gamma_d^{(UC)} - \Gamma_d^{\Sigma})/\Gamma_d^{\Sigma}$ for uncorrelated (green circles) fluctuations are plotted versus the coupling strength for the dephasing fluctuations γ_x for a fixed $\gamma_z = 0.2$ and for three temperature.

[2] cannot simply be extended to treat our model (2) and (3). The Niba uses the fact that a strong system-bath coupling tends to localize the system in a basis determined by the systems coupling operator. If two independent bath couple via two noncommuting system operators this assumption fails. Thus, we employ a numerical approach. The QUAPI approach is based on a symmetric Trotter splitting of the short-time propagator $\mathcal{K}(t_{k+1}, t_k)$ (describing time evolution over a time slice δt) for the full Hamiltonian H. The splitting is by construction exact in the limit $\delta t \to 0$, but introduces a finite Trotter error for a finite time increment, which has to be eliminated by choosing δt small. The QUAPI scheme further employs an approximated Feynman-Vernon influence functional which includes only nonlocal time correlations between observables in a time window $\tau_{\text{mem}} = k_{\max}\delta t$. Thus valid results are achieved by finding convergence while increasing τ_{mem} but at the same time decreasing δt to minimize the Trotter error. In the following, only converged results are presented and discussed. For a discussion to achieve convergence see Refs. [25,26].

V. RESULTS–SUPPRESSED OVERDAMPING

Weak dissipation at finite temperature by any environment results in exponentially decaying coherences for a TSS, i.e., $P_z(t) = \cos(\Delta t)e^{-\Gamma_d t}$ with dephasing rate Γ_d. With increasing system-bath coupling strength the dephasing rate increases until the dynamics turns overdamped and (small) additional dynamically behavior (as used in our fit function) emerges. This overdamping is a fingerprint of strong system-bath coupling.

We studied the coherent dynamics of a TSS with an relaxational bath with fixed coupling strength $\gamma_z = 0.2$ at temperature $T = 2\Delta/k_B$ and analyzed the dephasing rate as function of additional pure dephasing fluctuations. Figure 1 shows the according dephasing rate as function of γ_x. Adding increasing uncorrelated (green circles) pure dephasing fluctuations results in a linear increase of the dephasing rate up to the largest studied coupling strength of $\gamma_x = 0.5$. No overdamping in the according $P_z(t)$ data is observed. In striking contrast, we observe overdamping when adding increasing fully correlated (red diamonds) pure dephasing fluctuations for $\gamma_x \gtrsim 0.25$. This is reflected in Fig. 1 by a decreasing dephasing rate after an increase for smaller γ_x.

Fully correlated fluctuations result from a single source, for which the total system-bath coupling strength actually is $\gamma = \gamma_x + \gamma_z$. Interestingly, overdamping is achieved for $\gamma \gtrsim 0.45$ and neither pure dephasing nor relaxational fluctuations alone of this strength would overdamp the dynamics (data not shown). We additionally determined the rates of the pure dephasing and the relaxational fluctuations alone and added these to obtain Γ_d^{Σ}. A linear increase with γ_x almost identical with the uncorrelated case is observed (blue + symbols in Fig. 1). Thus, the overdamping observed is not an affect of any of the two fluctuations being strong enough but of the correlations between them.

Similar behavior is observed at lower temperatures. Figure 2 shows the ratios $(\Gamma_d^{(UC)} - \Gamma_d^{\Sigma})/\Gamma_d^{\Sigma}$ and $(\Gamma_d^{(FC)} - \Gamma_d^{\Sigma})/\Gamma_d^{\Sigma}$ versus γ_x for three different temperatures. For $T = 2\Delta/k_B$ (dashed lines) we again observe the sharp decline of the dephasing rate at $\gamma_x \gtrsim 0.25$. The same decline is observed at $T = \Delta/k_B$ (dotted line) at $\gamma_x \gtrsim 0.35$ and for $T = 0.5\Delta/k_B$ (full lines) we do not observe such a sharp decline within the studied γ_x range. Before the sharp decline of the dephasing rate we find in both, the uncorrelated and the fully correlated, cases deviations from the additive behavior in a range of $\pm 5\%$ which is nonmonotonic over the studied γ_x range. For temperatures $T < 0.5\Delta/k_B$ we observe deviations, i.e., reductions, of $\Gamma_d^{(UC)}$ to roughly 10% below Γ_d^{Σ}.

The same behavior is observed for smaller γ_z but the coupling strengths to reach overdamping increase and, thus, quickly drop out of the regime we are able to study. For $0.2 < \gamma_z \leqslant 0.5$ the results are very similar to the given data and overdamping is reached for $\gamma_x \gtrsim 0.2$.

Figure 3 shows the dephasing rates for a fixed coupling strength of the pure dephasing fluctuations, i.e., $\gamma_x = 0.5$, and increasing relaxational fluctuations. For lowest $\gamma_z \lesssim 0.01$ all three cases show identical behavior. For further increasing γ_z, both Γ_d^{Σ} and Γ_d^{UC} show linear increasing behavior. Again, adding fully correlated relaxational fluctuations shows strikingly different behavior. The dephasing rate decreases strongly, roughly by a factor of 2. Surprisingly, for $0.01 \lesssim \gamma_z \lesssim 0.2$ the dephasing rate decreases although $P_z(t)$ exhibits

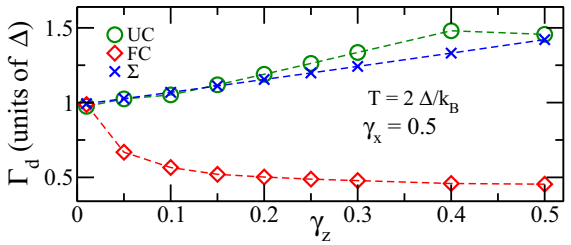

FIG. 3. The dephasing rates $\Gamma_d^{(FC)}$ for fully correlated (red diamonds) and $\Gamma_d^{(UC)}$ for uncorrelated (green circles) fluctuations and Γ_d^{Σ} (blue plus symbols) are plotted versus the coupling strength for the relaxational fluctuations γ_z for a fixed $\gamma_x = 0.5$ and a high temperature $T = 2\Delta/k_B$.

an initial oscillation minimum and full overdamping is not reached. Overdamped dynamics is observed only for $\gamma_z \gtrsim 0.2$. Thus, the fully correlated relaxational fluctuations suppress the dephasing of the pure dephasing fluctuations even when the dynamics is not fully overdamped yet. In Fig. 4 we have plotted $P_z(t)$ versus time to highlight the actual dynamic behavior of the cases for which we discussed the rates in Fig. 3. The same behavior is also observed for lower temperatures and smaller fixed γ_x but the suppression starts at larger γ_z.

VI. RESULTS–SUPPRESSED RELAXATION

Pure dephasing fluctuations alone cannot cause relaxation. Only relaxational fluctuations allow energy exchange between TSS and bath leading for weak dissipation at finite temperature to an exponential decay towards thermal equilibrium occupation numbers, i.e., $P_x(t) = P_x(0)e^{-\Gamma_r t} + P_x^{(eq)}(1 - e^{-\Gamma_r t})$. With this functional form we are able to fit all according numerical data for $P_x(t)$ and to extract the relaxation rate Γ_r. Figure 5 shows the relaxation rate $\Gamma_r^{(FC)}$ for fully correlated (red diamonds) and $\Gamma_r^{(UC)}$ for uncorrelated (green circles) fluctuations plotted versus the coupling strength for the relaxational fluctuations γ_z for a fixed $\gamma_x = 0.5$. Additionally, Γ_r^{Σ} is shown by the blue plus symbols. $\Gamma_r^{(FC)}$ (red full line) and $\Gamma_r^{(UC)}$ (green dashed line) are furthermore plotted versus the coupling strength of purely dephasing fluctuations γ_x for a fixed $\gamma_z = 0.5$. In all cases, temperature is $T = 2\Delta/k_B$.

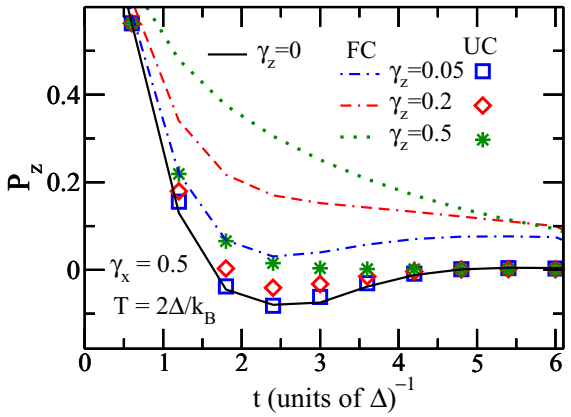

FIG. 4. $P_z(t)$ versus time is shown for fixed coupling strength $\gamma_x = 0.5$ of pure dephasing fluctuations at temperature $T = 2\Delta/k_B$ and for various coupling strengths γ_z for relaxational fluctuations.

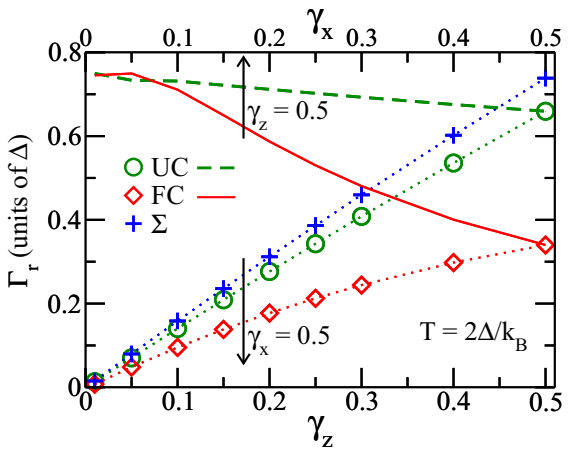

FIG. 5. The relaxation rates $\Gamma_r^{(FC)}$ for fully correlated (red diamonds) and $\Gamma_r^{(UC)}$ uncorrelated (green circles) fluctuations and Γ_r^{Σ} (blue plus symbols) are plotted versus the coupling strength for the relaxational fluctuations γ_z (lower three curves) for a fixed $\gamma_x = 0.5$ and versus the coupling strength of purely dephasing fluctuations γ_x (upper two curves) for a fixed $\gamma_z = 0.5$. The temperature is $T = 2\Delta/k_B$.

The relaxation rate $\Gamma_r^{\Sigma} = \Gamma_{r/d}^{\mathrm{SBM}}(\gamma_x = 0, \gamma_z)$ (note that $\Gamma_r^{\mathrm{PDM}}(\gamma_x, \gamma_z = 0) = 0$) increases linearly with γ_z (blue + symbols in Fig. 5) in the studied range of coupling strengths which reflects a dominating lowest order effect in the coupling to the relaxational bath. Additional strong but uncorrelated purely dephasing fluctuations with $\gamma_x = 0.5$ surprisingly, diminish this linear increase (see green circles in Fig. 5). The relaxation rate still increases almost linearly with γ_z but shows roughly a 10% reduction below Γ_r^{Σ}. A much weaker even sub-linear increase is observed when purely dephasing and relaxational fluctuations are fully correlated. At strongest investigated coupling, i.e., $\gamma_z = 0.5 = \gamma_x$, a reduction of the relaxation rate by a factor of 2 is observed.

Thus, purely dephasing fluctuations suppress relaxation. This is highlighted by the green dashed line in Fig. 5 which shows the relaxation rate due to a relaxational bath with $\gamma_z = 0.5$ versus the coupling strength γ_x to an additional uncorrelated pure dephasing noise source. A clear roughly linear decrease of the relaxation rate is observed with increasing γ_x. A much stronger suppression of relaxation is achieved by fully correlated pure dephasing fluctuations (red full line in Fig. 5).

At lower temperatures we observe qualitatively the same behavior but the suppression of the relaxation is quantitatively smaller. Figure 6 plots the ratio $\Gamma_r^{(UC)}/\Gamma_r^{\Sigma}$ and $\Gamma_r^{(FC)}/\Gamma_r^{\Sigma}$ versus γ_x for three different coupling strengths Γ_z at a low temperature of $T = 0.2\Delta/k_B$. With increasing dephasing fluctuations we observe a monotonic reduction of the relaxation rate. The effect is roughly a factor of 2 stronger for fully correlated fluctuations. An increase of the reduction is observed with increasing γ_z.

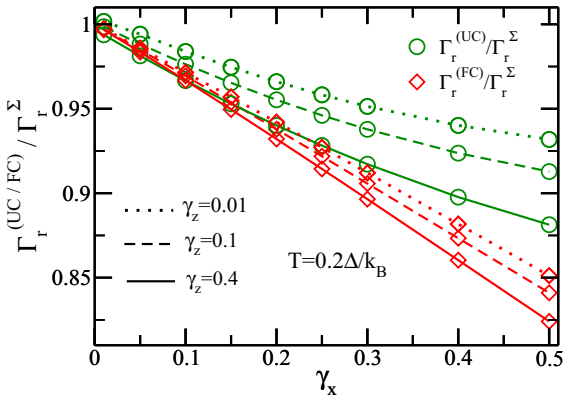

FIG. 6. The ratio $\Gamma_r^{(UC)}/\Gamma_r^{\Sigma}$ (green circles) and $\Gamma_r^{(FC)}/\Gamma_r^{\Sigma}$ (red diamonds) are plotted versus the coupling strength for the dephasing fluctuations γ_x three coupling strength γ_z at temperature is $T = 0.2\Delta/k_B$.

VII. CONCLUSION

In summary, we have investigated the influence of noncommuting fluctuations on the dissipative non-equilibrium dynamics of a quantum system at finite temperatures $T \simeq \Delta/k_B$. Using the numerical exact quasiadiabatic path integral approach we determined the dissipative dynamics of a quantum two-state system under the influence of a relaxational as well as an purely dephasing noise source and extracted the relaxation and dephasing rates.

We observe a decrease of the relaxation rate when purely dephasing fluctuations are increased. Thus, dephasing fluctuations suppress relaxation. This effect is enhanced substantially when both fluctuations, i.e., the relaxational and purely dephasing ones, are fully correlated or in other terms stem from the same physical origin. In contrast, dephasing rates are always increased by increasing any of the two fluctuations. However, fully correlated fluctuations result in overdamping at a lower total system-bath coupling than uncorrelated noncommuting fluctuations do. This, in turn, allows us to increase the dephasing rate by adding an additional independent noncommuting noise source in a two-state system beyond what is possible by increasing the system-bath coupling of a single dephasing source.

Our findings emphasize that even weak secondary noise sources cannot simply be neglected nor their influence be treated additive to the dominant dissipative influence when the two environmental noise sources couple to a quantum system via noncommuting operators. This, in turn, complicates accurate characterization of noise sources disturbing, for example, qubits.

ACKNOWLEDGMENT

T.P. and P.N. acknowledge financial support by the Deutsche Forschungsgemeinschaft (Project No. NA394/2-1).

[1] A. O. Caldeira and A. J. Leggett, Phys. Rev. Lett. **46**, 211 (1981).
[2] A. J. Leggett, S. Chakravarty, A. T. Dorsey, M. P. A. Fisher, A. Garg, and W. Zwerger, Rev. Mod. Phys. **59**, 1 (1987).
[3] U. Weiss, *Quantum Dissipative Systems* (World Scientific, Singapore, 1998), 2nd ed.
[4] H.-P. Breuer, E.-M. Laine, J. Piilo, and B. Vacchini, Rev. Mod. Phys. **88**, 021002 (2016).
[5] Y. Makhlin, G. Schön, and A. Shnirman, Rev. Mod. Phys. **73**, 357 (2001).
[6] V. May and O. Kühn, *Charge and Energy Transfer Dynamics in Molecular Systems* (Wiley-VCH, Weinheim, 2011).
[7] W. Wernsdorfer and R. Sessoli, Science **284**, 133 (1999).
[8] H. Grabert, P. Schramm, and G.-L. Ingold, Phys. Rep. **168**, 115 (1988).
[9] G. D. Mahan, *Many-Particle Physics* (Kluwer Academic / Plenum, New York, 1981).
[10] T. Fujisawa, T. Hayashi, and S. Sasaki, Rep. Prog. Phys. **69**, 759 (2006).
[11] M. Allen, J. Martin, and A. Yacoby, Nat. Commun. **3**, 934 (2012).
[12] R. P. Feynman and F. L. Vernon Jr., Ann. Phys. (NY) **24**, 118 (1963).
[13] P. Nalbach, J. Eckel, and M. Thorwart, New J. Phys. **12**, 065043 (2010).
[14] A. H. Castro Neto, E. Novais, L. Borda, G. Zaránd, and I. Affleck, Phys. Rev. Lett. **91**, 096401 (2003).
[15] C. Guo, A. Weichselbaum, J. von Delft, and M. Vojta, Phys. Rev. Lett. **108**, 160401 (2012).
[16] H. Kohler, A. Hackl, and S. Kehrein, Phys. Rev. B **88**, 205122 (2013).
[17] M. T. Mitchison and M. B. Plenio, New J. Phys. **20**, 033005 (2018).
[18] T. Palm and P. Nalbach, Phys. Rev. A **96**, 032105 (2017).
[19] H. Maguire, J. Iles-Smith, and A. Nazir, Phys. Rev. Lett. **123**, 093601 (2019).
[20] H.-G. Duan and M. Thorwart, J. Phys. Chem. Lett. **7**, 382 (2016).
[21] H.-G. Duan, R. J. D. Miller, and M. Thorwart, J. Phys. Chem. Lett. **7**, 3491 (2016).
[22] H.-G. Duan, P. Nalbach, R. J. D. Miller, and M. Thorwart, J. Phys. Chem. Lett. **10**, 1206 (2019).
[23] N. Makri, Chem. Phys. Lett. **193**, 435 (1991).
[24] N. Makri and D. E. Makarov, J. Chem. Phys. **102**, 4600 (1995).
[25] N. Makri and D. E. Makarov, J. Chem. Phys. **102**, 4611 (1995).
[26] T. Palm and P. Nalbach, J. Chem. Phys. **149**, 214103 (2018).
[27] T. Palm and P. Nalbach, J. Chem. Phys. **150**, 234108 (2019).